ACS CHEMICAL HEALTH & SAFETY

pubs.acs.org/acschas
Article

Potential Penetration of Engineered Nanoparticles under Practical Use of Protective Clothing Fabrics

Natalie Ireland, Yi-Hsuan Chen, and Candace Su-Jung Tsai*

Cite This: ACS Chem. Health Saf. 2024, 31, 393−403
Read Online

ABSTRACT: The commercial application of engineered nanoparticles (ENPs) has rapidly increased as their unique properties are useful to improve many products. ENPs, however, can pose a major health risk to workers through exposure routes such as inhalation and dermal contact. Research is lacking on the protective nature of lab coats when challenged with ENPs. This study investigated multiwalled carbon nanotubes (CNTs), carbon black (CB), and nano aluminum oxide (Al_2O_3) penetration through four types of lab coat fabrics (cotton, polypropylene, polyester cotton, and Tyvek). Penetration efficiency was determined with direct reading instruments. The front and back of contaminated fabric swatches were further assessed with microscopy analysis to determine fabric structure with contaminated and penetrated particle morphology and level of fabric contamination. Fabric thickness, porosity, structure, surface chemistry, and ENP characteristics such as shape, morphology, and hydrophobicity were assessed to determine the mechanisms behind particle capture on the four common fabrics. CNTs penetrated all fabrics significantly less than the other ENPs. CNT average penetration across all fabrics was 1.83% compared to 15.74 and 11.65% for CB and Al_2O_3, respectively. This can be attributed to their fiber shape and larger agglomerates than those of other ENPs. Tyvek fabric was found to be the most protective against CB and Al_2O_3 penetration, with an average penetration of 0.06 and 0.11%, respectively, while polypropylene was the least protective with an average penetration of 40.36 and 15.77%, respectively. Tyvek was the most nonporous fabric with a porosity of 0.50, as well as the most hydrophobic fabric, explaining the low penetration across all three ENPs. Polypropylene is the most porous fabric with a porosity of 0.77, making it the least protective against ENPs. We conclude that porosity, fabric structure, and thickness are more important fabric characteristics to consider when discussing particle penetration through protective clothing fabrics than surface chemistry.

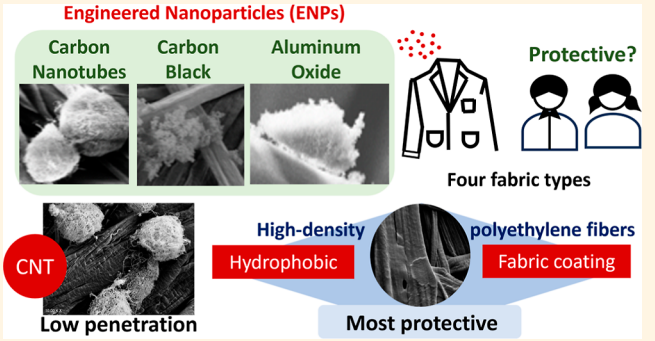

KEYWORDS: *Tyvek, polyester cotton, polypropylene, cotton, penetration, engineered nanoparticle (ENP), filtration efficiency*

INTRODUCTION

Dermal absorption and inhalation of engineered nanoparticles (ENPs) are the most common routes of ENP exposure for workers.[1,2] Protective clothing can protect against the deposition of ENPs onto skin and street clothing, which would limit subsequent resuspension from the contaminated skin or street clothing and inhalation of ENPs. The Center for Disease Control and Prevention (CDC) and the National Institute of Occupational Safety and Health (NIOSH) recommend wearing long pants and long-sleeved shirts, lab coats not made from cotton woven material, nitrile gloves, closed-toe shoes, and safety goggles when working with engineered nanoparticles (ENPs).[3] Lab coats are important protective measures against human exposure to ENPs when other administrative and engineering controls are insufficient. It is important to wear a lab coat with high capture efficiency and low penetration that is comfortable to wear for the duration of a shift when working closely with ENPs. Determining the most effective type of protective lab coat fabric against ENP penetration is important to consider when implementing a nanomaterial safety program.

Previous studies have shown that ENP contamination and resuspension for certain fabrics are substantial, causing secondary exposure. A study by Tsai[4] found that cotton fabric experienced the highest contamination and release of aluminum oxide nanoparticles, while polyester released the least amount of nanoparticles, concluding that cotton is not a suitable fabric for protection against nanoparticle inhalation exposure. The follow-up study by Maksot et al.[5] reported large

Received: March 7, 2024
Revised: May 29, 2024
Accepted: July 10, 2024
Published: July 18, 2024

https://doi.org/10.1021/acs.chas.4c00021
ACS Chem. Health Saf. 2024, 31, 393−403

amounts of ENP adhesion and release from four tested fabrics (polypropylene, Tyvek, cotton, and polyester cotton), with cotton fabric releasing the highest amount of ENPs after shaking, contributing to secondary exposure. Licina and Nazaroff[6] also found that clothing can serve as a vector for transporting small aerosols from one location to another, increasing the chance of airborne particle inhalation for humans. It is evident based on previous studies that clothing and other fabrics can be highly contaminated with ENPs, and these particles can be released into the environment or penetrate through the fabric, leading to inhalation or dermal exposure.

The hazards and toxicity related to ENP dermal exposure and absorption have not been extensively researched. Skin exposure to ENPs through protective clothing is of concern with regard to penetration potential, particularly in a dusty work environment. If ENPs are able to penetrate through protective clothing fabric and settle onto the skin, this can potentially cause ENP absorption through the skin, which could cause localized skin inflammation and an immune response.[7−9] Some researchers disagree about whether ENPs are able to penetrate through the stratum corneum of the skin.[10−14] If ENPs can penetrate the protective skin layers, then systemic availability of the ENP within the body will depend on the physical and chemical properties of the specific ENP.[15,16] The ability of ENPs to penetrate through the skin and become bioavailable throughout the body is an important point to consider when determining the level of protection necessary for protective clothing fabric for workers who routinely handle ENPs with known toxicities to the human body.

Most individual ENPs can be captured onto media by diffusion due to the stronger Brownian motion associated with their smaller size than their large agglomerates. Brownian motion increases the likelihood that a small particle will collide with and stick to fiber, while larger particles would be captured onto media by interception.[17−19] ENP agglomeration increases the mobility diameter of the ENP as it passes through the fabric material, and the capturing mechanisms are more likely to involve interception and impaction. Studies have shown that agglomerated ENPs penetrate less compared to spherical ENPs with equal mobility diameters due to the increased interception length of the agglomerates.[20,21] Brownian motion and interception are the governing mechanisms surrounding ENP capture onto fabric fibers.

Several previous studies have tested the penetration and filtration efficiencies of fabrics commonly used as lab coats or masks against ENPs under a wide range of conditions.[17,22−26] Studies challenging cotton fabric and masks with polydisperse sodium chloride (NaCl) aerosols found that cloth face masks and cotton clothing items experienced 40−90% penetration, while cotton material with higher thread counts and tighter weaves experienced lower penetration percentages compared to cotton materials with a lower thread count and looser weaves. Cotton fabric can vary in physical properties, which may affect fabric efficiency.[25,26] Golanski et al.[17] tested nonwoven polypropylene, cotton, and Tyvek fabrics against graphite nanoparticles sized between 10 and 100 nm, and observed the highest penetration percentages were for cotton fabric and the lowest was for Tyvek; however, the authors, Golanski et al., focused only on a narrow size range and only one type of nanoparticle, which does not represent practical exposure scenarios in work environments. This study builds upon previous work by capturing a wide range of working conditions, environments, and exposure scenarios where workers may be exposed to different types of nanoparticles and determine the most protective lab coat fabrics for most situations.

Fabric characteristics such as fiber and fabric thickness, porosity, fiber diameter, hydrophobicity, and packing density play a major role in determining the filter efficiency and penetration percentages of common lab coats.[5,22,27−29] The four fabric types chosen for this study represent commonly used lab coats for protection against ENP exposure with varying physical characteristics. ENP characteristics also play an important role in the penetration and filtration efficiency of the fabrics. The ENPs tested in this study were chosen as challenge aerosols due to their differing properties and wide use in the industry. CNTs are used in a wide range of industries and have many promising applications. Studies have determined many practical uses for CNTs. For example, CNTs were shown to successfully adsorb heavy metals and organic dye from water.[30] CNT particles have a wide range of applications in the electronics industry, CNTs have been used to transmit electrical signals, and research is being conducted on the application of CNTs for flexible electronics.[31] CB nanoparticles, traditionally used in printer ink and toners, have also been used to improve renewable energy harvesting, electrochemical devices, water sterilization methods, and remediation of petroleum and heavy-metal-contaminated soils.[32−35] Aluminum oxide nanoparticles have wide used in biotechnology and biomedicine.[36−38] Aluminum oxide nanoparticles also have promising applications in nano diesel fuel technology and as an adsorbent for the removal of mercury from waterways.[39,40]

To date, no systematic study has been conducted to evaluate the filtration efficiency of four types of fabrics commonly used as lab coats against three types of ENPs involving agglomerates and individual ENPs representing real-time exposure scenarios. This study aims to quantitatively evaluate penetration percentages of commonly available protective clothing (with fabric made of Tyvek, cotton, polypropylene, and polyester cotton) with ENPs (CNT, CB, and Al_2O_3) to inform those who routinely interact closely with different ENPs on the most effective protective clothing to wear. This research also aims to elucidate the mechanisms behind particle capture of spherical and nonspherical ENPs on different types of protective fabrics and the role fabric characteristics play in particle capture mechanisms. The study by Maksot et al.[5] first tested the same protective clothing fabric and ENPs to discover the amount of secondary resuspension after shaking each lab coat fabric and found that cotton fabric released the highest number of ENPs, while Tyvek trapped the highest amount of nano aluminum oxide and carbon black (CB) nanoparticles. The study by Hiyoto et al.[28] studied the same protective clothing fabric and ENPs to discover the effects of fabric surface changes on fabric contamination and found that plasma-treated fabrics experienced lower amounts of nanoparticle contamination and release for nano aluminum oxide and CB.

METHODS

Materials. Three different types of ENPs and four different types of protective clothing were evaluated in this study. Multiwalled carbon nanotubes (MWCNTs), nano aluminum oxide (Al_2O_3), and CB were chosen as they are common ENPs used in industries and whose properties differ from each other.

https://doi.org/10.1021/acs.chas.4c00021
ACS Chem. Health Saf. 2024, 31, 393−403

The MWCNTs were obtained from Nanolab (Waltham, MA, purity > 95%), with a primary diameter between 10 and 30 nm, and lengths ranging from 1 to 20 μm. CNT fibers are composed of 98.92% carbon, 0.14% sulfur, and 0.94% iron. Specific CNT fibers are produced through vapor deposition. CNT fibers are characterized as water insoluble and therefore hydrophobic.[41] Al_2O_3 nanoparticles were obtained from Nanophase Technologies Corporation (Romeoville, IL, purity 100%), with an average primary size of 40 nm. Al_2O_3 nanoparticles have a specific surface area of around 20 m^2/g with high hardness and high dimensional stability with no surface charge.[42] CB nanoparticles were Printex grade (Orion, purity 100%), with an average size of 40 nm. The particles have an average density of 1.70−1.90 g/cm^3 and are insoluble in water. They are also nonconductive particles that do not carry a charge.[43] CNTs and CB are carbon-based and hydrophobic; however, they differ in size and shape.[28] CNTs can be characterized by having an aspect ratio of greater than 3:1,[44] while CB is spherical. Al_2O_3 is hydrophilic and spherical shaped.

Four common types of lab coats tested included both woven and nonwoven fabrics. The woven fabrics included cotton (Fashion Seal men's lab coat) with a twill weave pattern and polyester cotton blend (80% polyester, 20% cotton, Red Kap women's button closure lab coat) with a combed plain woven weave pattern. The nonwoven fabrics included polypropylene spun bond (Keystone HD polypropylene lab coat) and polyethylene spun bond (DuPont Tyvek). The lab coats were purchased through a commercial vendor (Global Industrial) of protective clothing in adult size, small. The polyester cotton blend was composed of 80% polyester and 20% cotton. The exact structure of the fabric blend is unknown; however, it can be concluded that the fabric consists of 80% hydrophobic and 20% hydrophilic fibers. The polypropylene fabric was composed of smooth and rough portions that were evenly distributed throughout the entire fabric. Swatches of polypropylene fabric 47 mm in length were evaluated; therefore, any additional finishing seen on parts of the fabric did not have an impact on the overall particle retention and penetration. The fabric properties of fiber size, fabric thickness, fabric structure, porosity, water contact angle (WCA), absorption rate, and water vapor transmission rate (WVTR) were determined for each fabric. Fabric structure, fiber size, thickness, WVTR, static WCA, and absorption rate were measured for each of the four fabrics in a previous study.[5] Porosity and pore volume were calculated for each fabric using equations from a previous study.[22] The calculations for each fabric porosity are located in the Supporting Information.

Facilities, Equipment, and Procedure. As seen in the schematic diagram of the experimental setup (Figure 1a), the research was conducted in a closed glovebox (89 × 61 × 64 cm) with a ventilated ultrafilter system (Terra Universal, Fullerton, CA, USA) to provide clean air with background aerosols ~10 particles/cm^3. Background aerosols were measured using direct reading instruments as a negative control in the test chamber. The fabric swatch was placed in a filter holder. The fabric test system in the glovebox ran overnight between each ENP trial, and then background particle levels inside the glovebox were measured. Background particle levels were determined to be negligible in both the 10−420 nm particle size range and the 0.3−10 μm particle (~10 particle/cm^3) for CNT and were corrected during CB and Al_2O_3 trials (<100 particle/cm^3). An enclosure made of

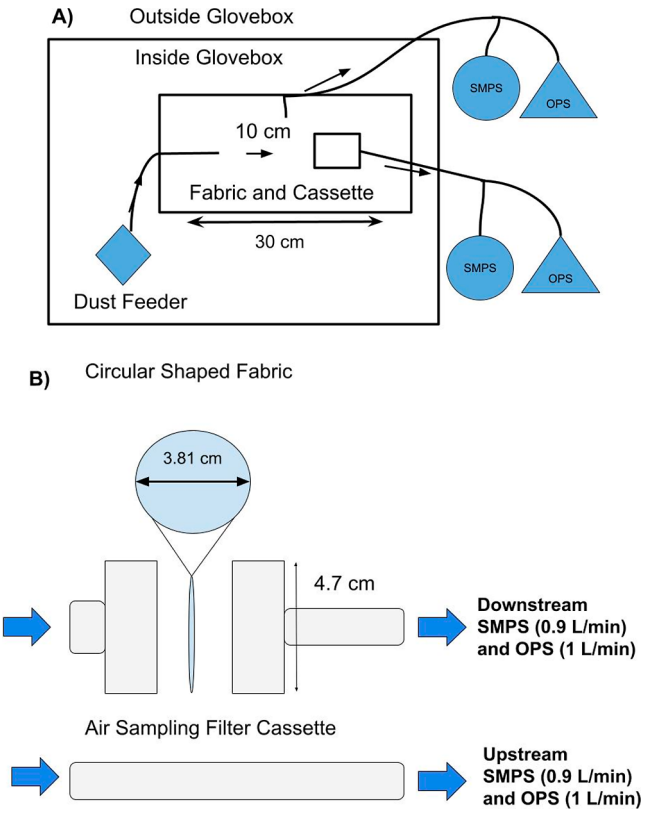

Figure 1. Schematic diagram of the experimental setup. (a) Diagram of the entire experimental setup. (b) Close-up diagram of the fabric inside the air sampling cassette.

acrylic plastic with a removable top was placed inside the glovebox to provide a second layer of containment during the experiment. The filter holder was then placed inside the enclosure for fabric testing. The aerosol generator used was a Wright Dust Feeder II (WDF II) (CH Technologies, USA). Two direct reading instruments (DRIs), the NanoScan Scanning Mobility Particle Sizer (SMPS) (TSI model 3910, Shoreview, MN, 10−420 nm) and the Optical Particle Sizer (OPS) (TSI model 3330, Shoreview, MN, 0.3−10 μm), were used to monitor and record aerosol concentrations. The WDF II was placed inside the glovebox and connected to the sampling enclosure with conductive tubing. The DRIs were placed outside the glovebox and connected to the sampling enclosure with conductive tubing. One set of DRIs was located 10 cm upstream of the filter cassette within the sampling enclosure, and the other set of DRIs was connected to the downstream end of the cassette, as shown in Figure 1a,b. A thermal anemometer (VelociCalc 9545, TSI, Shoreview, MN) measured humidity and temperature at 46−48% and 75−75.4 °F, respectively. These measurements are in line with the average relative humidity and temperature in a laboratory environment where ENPs may be manufactured or used. Particle number concentrations and size distributions were measured both upstream and downstream using two DRIs each, as shown in Figure 1a.

Fabric Preparation. Before fabric swatches were prepared, the surfaces of the tools and lab benches were wiped off with isopropyl alcohol and deionized water. Each fabric swatch was cut into a circular shape with a diameter of about 3.81 cm. The fabric swatches were then placed in clean Petri dishes and transferred to the glovebox. Each fabric was placed in a 47 mm

https://doi.org/10.1021/acs.chas.4c00021
ACS Chem. Health Saf. 2024, 31, 393−403

Table 1. Measured Descriptive Properties of the Four Fabrics Tested

fabric	fabric structure[a]	fiber size[a] (μm)	thickness[a] (mm)	WVT[a] (g/m^2 × day)	porosity	static WCA[a]	absorption rate[a] (μL/s)	pore volume (m^3/kg)
cotton	twill woven	18.10 ± 1.40	0.66 ± 0.01	7561 ± 196	0.66		18.90 ± 1.20	0.0010
polyester cotton	plain woven	polyester = 12.00 ± 0.80 cotton = 21.50 ± 2.50	0.41 ± 0.01	7070 ± 561	0.60		4.24 ± 0.25	0.0010
Tyvek	non woven	single fiber = 13.90 ± 1.40 entire fabric = 28.20 ± 7.10	0.15 ± 0.01	3216 ± 61	0.50	125.90 ± 1.50		0.0011
polypropylene	non woven	29.20 ± 3.50	0.25 ± 0.01	6121 ± 149	0.77	121.7 ± 2.10		0.0037

[a]Data was obtained from Maksot's study.[5]

in-line filter holder (Pall Corp., Port Washington, NY, USA) and secured flat covering the entire opening of the filter holder, as shown in Figure 1b. Before the experiment, clean air was run over each fabric swatch for 30 min to clean the fabric from any loose fibers and ensure the downstream concentration did not contain a significant amount of fabric particles.

Aerosolization of ENPs. The WDF II was packed with ENPs and manually stamped before each trial. Clean air was pumped through the dust feeder at a rate of 20 psi, while the WDF II was operated at a speed of 2.00−4.00 rpm. The NanoScan SMPS and OPS ran at a sampling flow rate of 0.9 and 1.0 L/min, respectively. The equipment was calibrated to the proper flow rates with a bubble calibrator prior to the beginning of the experimental trials. Together, the instruments measured particles ranging from 10 nm to 10 μm with a collective sampling flow rate of 1.90 L/min. Based on these parameters, the face velocity was calculated as 2.78 cm/s and associated with minimal pressure drop on the fabric. The face velocity is low in order to simulate air passing through protective clothing while a person is wearing protective clothing. The dust feeder was run for an average of 10 min before data collection began for particle concentrations to stabilize post the initial startup of the dust feeder that caused fluctuation. After the initial 10 min, upstream and downstream data were collected for 30 min. Over the entire 30 min sampling period, downstream concentrations were consistent for each fabric when challenged with the same ENP. This suggests loading of the nanoparticles onto the fabric over time is not a factor affecting penetration, meaning loading onto the fabric did not significantly impact downstream concentrations of nanoparticles and did not play a role in overall penetration percentages. Each fabric trial was replicated three times under the same operating conditions. The enclosure inside the glovebox was wiped down with deionized water, and the outside surface of the conductive tubing was wiped with Sani wipes between each of the trials to minimize background concentrations. Penetration was determined by comparing the upstream concentration, U, to the downstream concentration, D, as $P = \left(\frac{D}{U}\right) \times 100\%$. Penetration was calculated for all particle sizes combined and for each particle size bin reported by the sampling instruments so as to determine the most penetrating particle size (MPPS) for each ENP across the different fabrics.

Studies have shown that the SMPS is most accurate with particle sizes between 20 and 200 nm, with an inaccuracy of ±10%. Particles larger than 200 nm were counted with an inaccuracy of ±30%, and particles smaller than 20 nm were counted with high inaccuracies as well.[45,46] Additionally, below 40 nm, the SMPS can count higher aerosol concentrations than are actually present.[47] For this reason, this investigation analyzed SMPS data between particle diameters of 36.5−154 nm, which is the most accurate data to investigate fabric penetration of nanoparticles. The average measured normalized particle concentration for all three ENPs is plotted in Figure S2, and described even further in Table 1. The peak particle size for aerosolized CNT was 64.9 nm, while the peak particle sizes for Al_2O_3 and CB were 86.6 and 154 nm, respectively.

Scanning Electron Microscopy Analysis. Both ENP-contaminated and clean fabric samples from each fabric type were analyzed by using scanning electron microscopy (SEM). Each fabric sample was taped to a substrate using carbon tape, coated with gold alloy, and imaged. The SEM images were used to compare the upstream versus downstream contamination of each piece of fabric and to compare the contaminated fabrics to the uncontaminated fabrics. Both front and back images were taken for each piece of fabric to compare and characterized.

Statistical Analysis. The ENP challenge concentrations were characterized as follows. Summary statistics of the penetration percentages were tabulated, including the coefficient of variation (CV), which was calculated in order to determine the dispersion around the means of the challenge aerosol concentrations. Two-way ANOVA analysis with interaction term was conducted to determine whether the penetration percentage differed between ENPs and fabrics. The assumptions for the two-way ANOVA were verified using the SMPS/OPS software package. Statistical analysis was conducted with the Stata BE software package (version 17.0, StataCorp, College Station, TX). At a 95% confidence level, p-values < 0.05 were considered statistically significant.

RESULTS AND DISCUSSION

Fabric Characteristics. The measured descriptive properties for each fabric are listed in Table 2. Fabric structure, fiber size, thickness, porosity, and pore volume provide insight into the specific fabric's ability to trap large and small particles. Thicker nonwoven fabrics with low porosity and large fiber size should have a higher particle capture efficiency when compared to fabrics without these characteristics. Tyvek fabric is the least porous, while cotton is the thickest fabric. Polypropylene is the most porous fabric. The static WCA and absorption rate measurements were used to determine the hydrophilicity or hydrophobicity of each fabric. Tyvek and polypropylene were hydrophobic, while polyester cotton and cotton were hydrophilic. Cotton fabric is the most porous fabric, with its absorption rate and WVTR higher than the

https://doi.org/10.1021/acs.chas.4c00021
ACS Chem. Health Saf. 2024, 31, 393−403

Table 2. Average Penetration Percentages over the 30 min Sampling Period of the Three Different ENPs on the Four Types of Lab Coats in the Size Range 36.5 nm to 10 μm (particles/cm^3)

ENP	lab coat fabric type	average penetration
carbon nanotubes	cotton	1.92 ± 0.74
	polyester cotton	2.21 ± 0.33
	polypropylene	1.61 ± 0.14
	Tyvek	1.59 ± 0.84
carbon black	cotton	3.17 ± 0.97
	polyester cotton	19.36 ± 7.59
	polypropylene	40.36 ± 10.31
	Tyvek	0.06 ± 0.02
aluminum oxide	cotton	17.66 ± 7.33
	polyester cotton	13.04 ± 5.37
	polypropylene	15.77 ± 3.49
	Tyvek	0.11 ± 0.05

other three fabrics. SEM images presenting the fabric structure for each noncontaminated fabric swatch are shown in Figure S1. The two woven fabrics (cotton and polypropylene) were composed of layers of individual fibers in a defined pattern. The Tyvek nonwoven fabric had no discernible individual fibers and instead consisted of multiple layers forming a consistent web of material, which was consistent throughout the fabric swatch. The polypropylene nonwoven material did not have a consistent pattern throughout, with some areas consisting of fibers with large gaps in between, while other areas were a consistent web of material. The SEM images support the data that polypropylene fabric is the most porous, with the highest pore volume.

Overall Penetration. The overall average penetration percentages are summarized in Table 2. The ANOVA results showed that ENP significantly impacted penetration, meaning that penetration varies based on the challenge ENP. There was an increase in penetration over all fabrics when challenged with CB and aluminum oxide compared to CNT, and CB penetration was significantly higher than CNT penetration throughout all four fabric types (p = 0.028, Table S2). CNT particles tend to form large agglomerates compared with the other two ENP types. This assumption is supported by SEM images in Figure 3, where each fabric type is capturing larger CNT agglomerates compared to aluminum oxide and CB. The downstream fabric images show aluminum oxide and CB causing a higher amount of individual particle contamination compared to CNT, where the particles tend to stick together.

The ANOVA results also showed that fabric type significantly impacted penetration, meaning that penetration varies based on the type of fabric being challenged (Table 3). Tyvek fabric experienced the least penetration when challenged with CB and aluminum oxide, while all fabrics were equally protective when challenged with CNT. Tyvek fabric was significantly better at blocking all types of ENPs compared to polypropylene fabric (p = 0.014, Table S3), while the data are suggestive that Tyvek is better at blocking particles compared to polyester cotton and cotton fabrics. The physical properties of Tyvek fabric make it very good at trapping particles. Tyvek is a very thin fabric with low porosity. Polypropylene has the highest porosity with large gaps between individual fibers, allowing more space for particles to pass through. The SEM images in Figure 3A4,B4,C4 clearly show

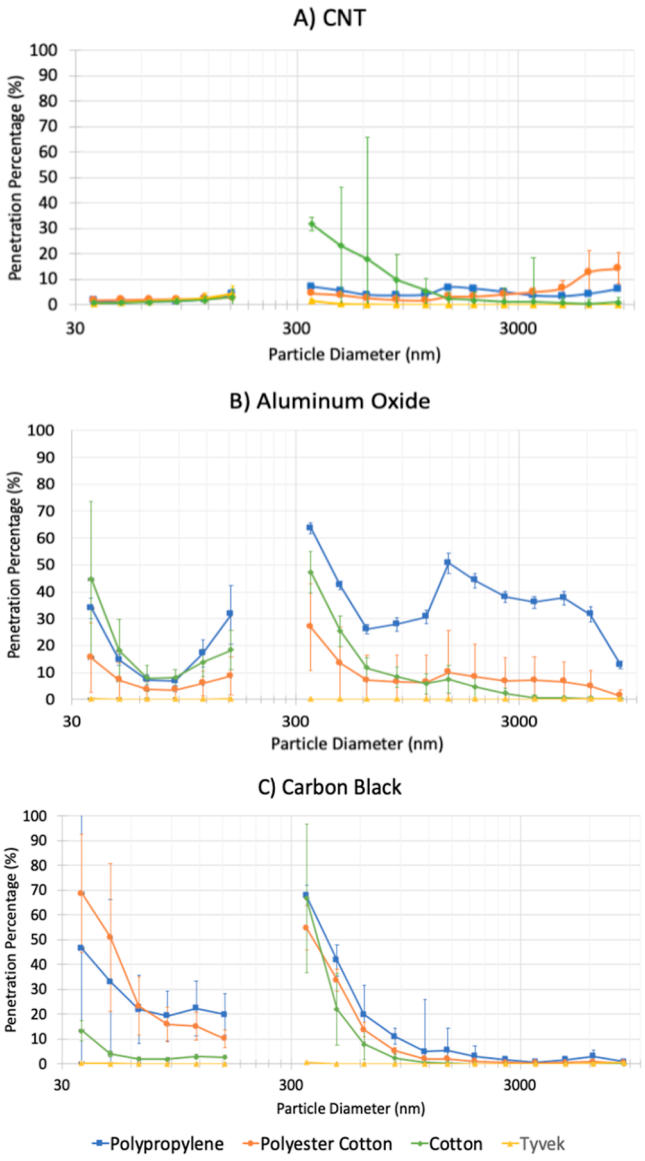

Figure 2. Size fractioned (36.5−8500 nm) penetration for each fabric against (a) CNT, (b) aluminum oxide, and (c) carbon black.

large gaps in the polypropylene fabrics and Tyvek fabric, capturing both large and small particles on the upstream side.

The ANOVA results showed a statistically significant interaction term, which means that the penetration of the different ENP particle types varies among fabrics (Table 3). A combination of ENP type and fabric type has a compounded effect on penetration compared to the two factors alone. Polypropylene challenged with CB had significantly higher penetration than all other fabrics when challenged with CNTs and aluminum oxide, and both Tyvek and cotton when challenged with CB (p < 0.05, Table S4). The results show that polypropylene, when challenged with CB is the least protective fabric. CB had the highest rate of aerosolization, while polypropylene had the highest porosity. Table S4 also suggests that Tyvek fabric is the most protective compared to the polypropylene fabric when challenged with CB since the mean difference is greater between Tyvek fabric and polypropylene.

Penetration by ENP and Particle Size. We further analyzed this to determine if the performance of different fabrics would vary significantly to the same ENP on different

https://doi.org/10.1021/acs.chas.4c00021
ACS Chem. Health Saf. 2024, 31, 393−403

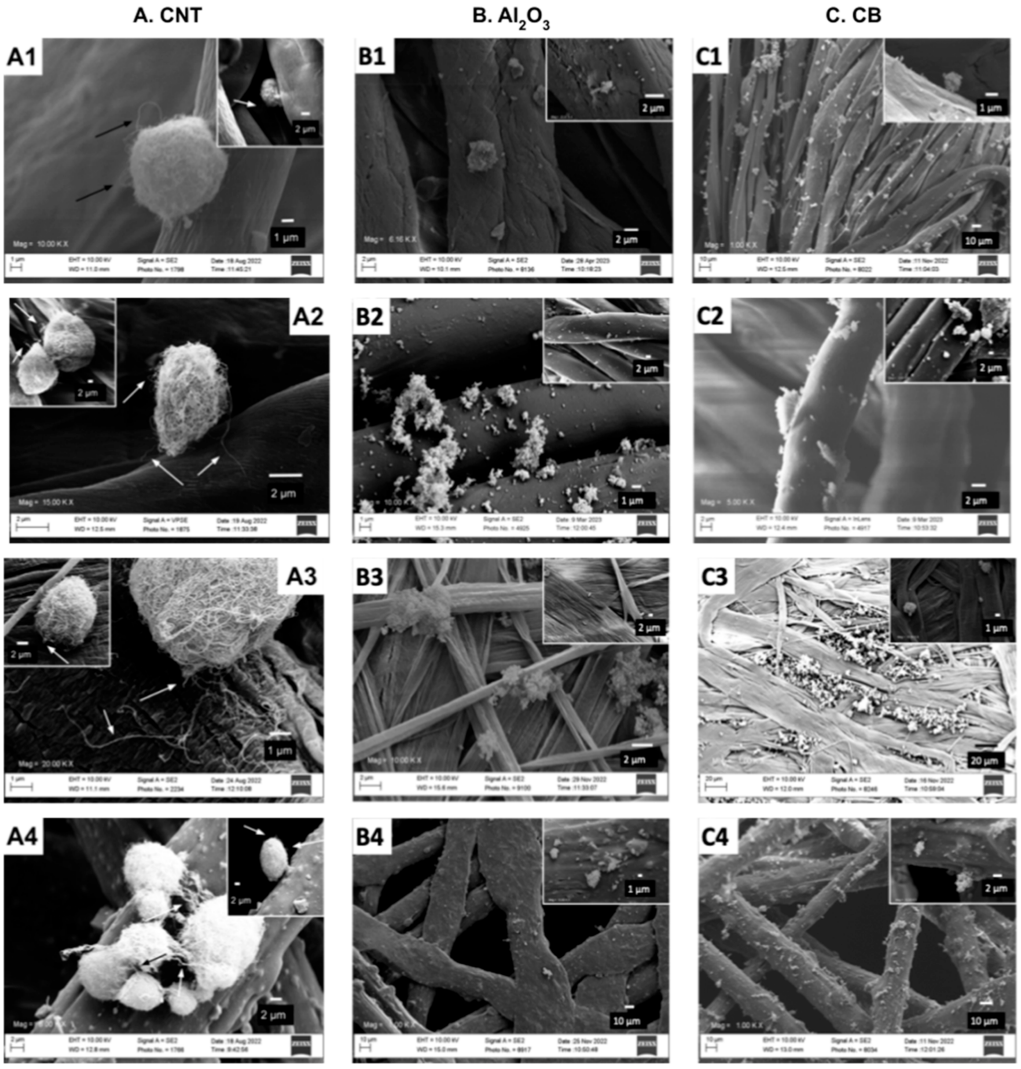

Figure 3. SEM images of the upstream shown in a large image and downstream shown in small inserted image. Sides of each of the four fabrics when challenged with CNT, aluminum oxide, and carbon black ENPs. (A) CNT, (B) aluminum oxide, (C) carbon black, in which (A1,B1,C1) are cotton fabric, (A2,B2,C2) are polyester cotton fabric, (A3,B3,C3) are Tyvek fabric, and (A4,B4,C4) are polypropylene fabric. The arrows show individual CNT fibers within the larger CNT agglomerations.

Table 3. Two-Way ANOVA Results Comparing the Interaction between the ENP and Fabric Type for the Penetration Percentages

	SS	d_f	MS	F	p-value
ENP	1226	2	613	9.39	0.0010*
fabric	1638	3	546	8.37	0.00060*
ENP*fabric	1997	6	333	5.10	0.0017*
residual	1566	24	65		
total	6428	35	184		

particle sizes. The particle size fractioned penetration percentages for each type of fabric, when challenged with each ENP across the size range 36.5 nm to 10 μm, were evaluated and are summarized in Figures 2, 3. Further ANOVA analysis was conducted and shows the interaction term between fabric, ENP, and size to be statistically significant, meaning penetration varies based on the combined effects of particle size, fabric, and ENP type (p = 0.033, Table S5). The smallest and largest particle sizes sampled by the SMPS as well as the smallest particle size sampled by the OPS were evaluated to depict a range of particle sizes.

CNT. Penetration percentages of CNTs against all four fabric types cross the range of 36.5−10,000 nm, are shown in Figure 2a. Overall, all four fabrics challenged with CNTs had very similar penetration percentages. The MPPS for all fabrics was 154 nm, with penetration percentages between 3 and 5%. This data suggests that all four fabric types are equally protective against CNT nanoparticles between the sizes 36.5−154 nm. ANOVA results suggest that the fabrics in this size range are not statistically different (Table S6). For larger CNT particles between 0.3 and 1 μm, the cotton fabric had the highest penetration percentages, at 31% in the 0.35 μm size, while all four fabric penetrations were below 20% for all other sizes. This is further supported by statistical analysis showing that cotton fabric penetration of CNTs at the 0.35 μm size is significantly higher than the other three fabrics (p = 0.05, Table S6). Since CNTs are hydrophobic, the particles tend to stick together and form very large agglomerates, usually greater than 10 μm. Agglomerates of CNTs approximately 100 nm to 20 μm were observed and captured on the surface of each fabric, as shown in Figure 3A1−A4.

https://doi.org/10.1021/acs.chas.4c00021
ACS Chem. Health Saf. 2024, 31, 393−403

Al_2O_3. The particle size-fractioned penetration percentages for each type of fabric, when challenged with Al_2O_3 across the range of 36.5−10,000 nm, are shown in Figure 2b. At 154 nm, the polypropylene fabric had the highest penetration of about 32%, followed by cotton (18%), polyester cotton (9.0%), and Tyvek (0.10%). The MPPS was 0.35 μm across the size range 0.3−1 μm for all fabrics, with polypropylene fabric having the highest penetration at 64%, followed by cotton (47%), polyester cotton (29%), and Tyvek (0.08%). The Tyvek fabric penetration was significantly lower compared to the other three fabrics (Table S7). ANOVA showed that fabric type does have a significant effect on penetration; however, particle size and the interaction term between fabric type and particle size do not significantly affect penetration (Table S7). Figure 3B1−B4 show upstream and downstream SEM images of each fabric type contaminated with Al_2O_3. Overall, polypropylene exhibited the most penetration of Al_2O_3 nanoparticles, most likely because polypropylene fabric has a high porosity, allowing particles to pass through the openings of the fabric more easily compared to fabrics with lower porosity.

CB. The size-fractioned particle penetration percentages for each type of fabric, when challenged with CB nanoparticles across the range of 36.5−10,000 nm, are shown in Figure 2c. The MPPS was 36.5 nm for all fabrics. There was also a slight increase in penetration at the 115.5 nm size for all fabrics except polyester cotton. At the 36.5 nm size, polyester cotton had the highest penetration at about 68%, followed by polypropylene (46%), cotton (13%), and Tyvek (0.30%). The penetration observed at this size range was significantly higher than at the size range 154 nm (Table S7). At the 115.5 nm size, polypropylene had the highest penetration at 22.40%, followed by polyester cotton (15%), cotton (3.0%), and Tyvek (0.06%). In the 0.3−1 μm size range, the MPPS was 0.35 μm for all fabrics. Polypropylene, polyester cotton, and cotton all had very similar penetration percentages at 68, 55, and 67%, respectively. Tyvek penetration at this size range was 0.60%. Tyvek fabric penetration was lower compared to the other three fabrics, and the data suggest that Tyvek is more protective than polypropylene (Table S8). ANOVA results show that both fabric and particle size independently affect penetration, but the interaction term between the two factors is insignificant (Table S8). Figure 3B shows upstream and downstream SEM images of each fabric type contaminated with CB. It is clear that Tyvek fabric allowed the lowest amount of particles to penetrate the fabric, while the other three fabrics experienced a higher degree of contamination on the downstream side, which is consistent with the observed penetration percentages.

Understanding Penetration Percentages. Using the data collected in this study along with each fabric's physical and chemical characteristics, the mechanisms by which each fabric captures particles can be elucidated. Since each ENP has different morphologies and surface characteristics, comparing the same fabric between different ENPs is helpful in determining if specific fabrics, each with their own properties, are more protective compared to others. Based on known fabric and ENP characteristics, mechanisms for particle capture on different fabrics can be determined. This can inform future decisions about lab coat fabrics based on the ENP being manufactured.

CNT particles do not significantly penetrate any fabric, possibly due to larger agglomerates. For Al_2O_3 particles, Tyvek is the most protective fabric, while polypropylene and cotton are the least protective fabrics. Polypropylene was the most porous fabric and experienced the most penetration overall. Figure 3B4 shows particle capture increases where the fabric is nonporous and the Al_2O_3 particles are able to settle; however, in areas where large gaps exist between the fibers, the particles pass through and settle onto skin or undergarments. Polypropylene fabric is extremely nonhomogeneous, where some are made of single fibers with large gaps in between. This makes the collection efficiency of polypropylene fabric varied as well. Tyvek was the most protective fabric against CB nanoparticles. These results are consistent with the known physical properties of each fabric. Cotton was the next most protective fabric. This result may be explained by the thickness of cotton trapping the slightly larger CB nanoparticle through interception.

Relationships between ENP Penetration and Fabric Type. Table 2 shows the penetration percentage of each fabric when challenged with each nanoparticle averaged over 30 min and three trials over the size range of 36.5 nm to 10 μm. The highest penetration overall occurred when the polypropylene fabric was challenged with CB nanoparticles, while the Tyvek fabric experienced the lowest penetration overall when challenged with CB. All four fabrics when challenged with CNTs experienced very low penetration, further characterizing CNT as the least penetrating nanoparticle for all fabrics. All fabrics have penetration percentages well under 20% when challenged with CNTs. It is clear that the main factors driving CNTs' low penetration are CNTs' stickiness and their ability to form large agglomerates. Figure 3A shows large agglomerates of CNTs collected on each of the four fabrics.

When considering the fabric penetration of CB and Al_2O_3, it is important to decipher which fabric and particle characteristics are the most important to fabric penetration. Looking at Figures 2 and 3, we can conclude that the polypropylene fabric had the highest particle penetration. This is mostly governed by the fabric's porosity. Polypropylene has the highest porosity, meaning the fabric consists of large gaps in between the woven parts of the fabric. Al_2O_3 nanoparticles also form agglomerates but less so when compared to CNT nanoparticles, and Al_2O_3 agglomerates easily deagglomerate. Tyvek fabric is the most efficient at capturing these particles, since most large and small particles are captured on the surface of the fabric, as shown in Figure 3C. However, many particles are able to pass through the large gaps in the polypropylene fabric. Similar effects of porosity were observed for the CB particles on each of the four fabrics. Interestingly, the cotton fabric exhibited a higher collection efficiency compared to the other woven fabric and polypropylene shown in Figure 3C. Cotton fabric is the thickest fabric with the second lowest porosity, which might be contributing to the low penetration of CB. For the Tyvek fabric, which is the most protective for CB nanoparticles, the nanoparticles can be seen accumulating and agglomerating onto the surface of the fabric in Figure 3C3. It can be observed that the particles settle onto each other, forming even larger agglomerates.

These results show that physical characteristics, such as a fabric's porosity or a particle's size and agglomeration rate matter more than certain chemical properties like hydrophobicity or surface charge. For both aluminum oxide and carbon black, ENP penetration follows a pattern: the most porous fabric experiences the most penetration, while the least porous fabric experiences the lowest penetration.

https://doi.org/10.1021/acs.chas.4c00021
ACS Chem. Health Saf. 2024, 31, 393−403

Polypropylene fabric was able to significantly capture more CNT particles than CB particles. Since CNT particles form fairly large agglomerates, the particles may be captured onto the fibers more easily than the smaller and more rounded CB particles. Tyvek was the most protective fabric over all three ENPs, which can be explained by the low porosity of the fabric. Nanoparticles, regardless of different physical and chemical morphologies, cannot move through the individual fibers of the Tyvek fabric well, causing the particles to attach and stick to the surface of the fabric. This finding further supports the previous conclusion that the physical characteristics of the fabric and particles have a larger effect on overall penetration compared with the surface chemical characteristics or hydrophobicity of fabric and particles.

Particle Deposition Mechanisms on Fabric. The total efficiency (E_Σ) of a filter can be calculated when each mechanical single fiber efficiency is known, given by eq 1[48]

$$E_\Sigma = 1 - (1 - E_R)(1 - E_I)(1 - E_D)(1 - E_{DR})(1 - E_G) \quad (1)$$

where E_R is the interception efficiency, E_I is the impaction efficiency, E_D is the diffusion efficiency, E_{DR} is the interception efficiency of the diffusing particles, and E_G is the settling efficiency. In practice, calculating total efficiency is more complicated when a range of particle sizes and fiber diameters are present. Each fabric is made of slightly different fibers, each with slightly different thicknesses and diameters, and particle sizes for each ENP ranged from 10 nm to 10 μm; it is difficult to predict the total efficiency of each fabric using eq 1. However, taking into account the peak particle sizes for each ENP and the face velocity of 2.78 cm/s, during the experiment the predominant mechanisms most likely governing the capture of particles for each ENP can be determined. For CNTs and Al_2O_3, the peak particle size was 64.9 and 86.6 nm, respectively, and the collection of particles was governed by diffusion, while the peak particle size for CB was 154 nm, and the collection of particles was governed by diffusion and interception.

The single fiber efficiency due to diffusion (E_D) is calculated as[48]

$$E_D = 2Pe^{-2/3} \quad (2)$$

where 2 is a coefficient determined empirically, and Pe is the dimensionless Peclet number defined in eq 3

$$Pe = \frac{d_f U_0}{D} \quad (3)$$

where d_f is fiber diameter, U_0 is the face velocity of the filter, and D is the particle diffusion coefficient. For the peak particle size of the CNT nanoparticle, the Peclet number and single fiber efficiency due to diffusion can be determined for each fabric by taking the average fiber size (0.0018 cm for cotton, 0.0017 cm for polyester cotton, 0.0014 cm for Tyvek, and 0.0029 cm for polypropylene), the face velocity of 2.78 cm/s, and the diffusion coefficient of 1.73×10^{-5} cm^2/s. Using eqs 2 and 3, for cotton fabric, the Pe is 291.3 and E_D is 0.046, for polyester cotton fabric, the Pe is 275.1 and E_D is 0.047, for Tyvek fabric, the Pe is 226.6 and E_D is 0.054, and for polypropylene fabric, the Pe is 469 and E_D is 0.033. Polypropylene fabric is determined to be the least efficient at capturing particles, while Tyvek is determined to be the most efficient for particles sized 64.9 nm. The efficiency calculation results were consistent with the general pattern found in the experimental results.

The single fiber efficiency equation (eq 2) focuses on one fiber in the middle of a filter that is positioned perpendicular to the airflow. Single fiber efficiency is a rate that can be determined by dividing the number of particles collected on the fiber in 1 s by the total number of particles that would have passed through the fiber area in 1 s.[48] This rate of efficiency assumes that all fibers in the filter have the same diameter and length. The efficiency of fabric is more complicated, due to the nonuniformity in fibers and different fiber efficiencies within the same piece of fabric. Dhaniyala and Liu[49] have proposed a theoretical model of filtration that takes into account filter inhomogeneity. This model considers variations in the packing density and pressure drops within the same piece of fabric. The total efficiency of each fabric can be better defined as eq 4

$$\eta_{total} = 1 - \int \frac{U(\alpha)}{\bar{U}}(1 - \eta(\alpha))g(\alpha, \sigma_g)d(\alpha) \quad (4)$$

where $U(\alpha)$ is the velocity in the media, $\bar{U}$ is the average face velocity, $\eta(\alpha)$ is the cell efficiency relating to solidity, $g(\alpha,\sigma_g)$ is the mean packing density calculated from the filter bulk properties, and $d(\alpha)$ is the packing density of a cell. Since most fabrics are inhomogeneous, this theoretical model is able to more accurately predict filtration efficiencies. A recent study utilized the inhomogeneous fibrous filtration theory and eq 4 to explain experimental results of particle penetration through the fabric.[23] Due to the nonuniformity of packing density between fabrics used for protective clothing, this causes different face velocities throughout the same swatch of fabric and different filter efficiencies within the same piece of fabric.

The basic deposition mechanisms rely on the single fiber efficiency theory, which may not accurately depict the type of ENP capture for lab coats but can elucidate the basic mechanisms of particle capture. Previous studies have used single fiber efficiency theories to predict the penetration of MWCNTs through screen filters. Wang, Kim and Pui[50] found that CNT penetration was less than the penetration of a sphere with an equal mobility diameter. They hypothesize that the CNT particles become deformed in the flow, leading to reduced interception length, which is proportional to the aerodynamic diameter. Ref 51 further investigates the application of the single fiber theory on MWCNT penetration through respirator filter media. CNT has lower penetration than NaCl particles of the same mobility diameter due to its elongated shape. This theory partly explains why CNT penetration was significantly lower compared to CB and Al_2O_3 through most fabrics. CNT fibers bend and agglomerate more readily than spherical particles, therefore getting trapped by the individual fibers of the fabrics.

Discussion of Hydrophobic and Hydrophilic Forces. The interactions between particles and fabrics with similar or opposing polarities along with the hydrophobicity versus hydrophilicity of each surface are important to consider when discussing particle capture by differing fabrics. There is evidence that a hydrophobic force attraction exists between two hydrophobic surfaces in an aqueous solution, while a repulsion exists between hydrophobic and hydrophilic surfaces.[52,53] Some evidence exists to support the theory that attractive forces between two hydrophobic surfaces exist when they are not in water. These forces are only seen at close distances with a decay length of 0.3−1.0 nm.[54] Maksot et al.[5] found that capillary forces may play a role in particle adhesion

https://doi.org/10.1021/acs.chas.4c00021
ACS Chem. Health Saf. 2024, 31, 393−403

to the surface of fabrics. Capillary forces are formed between an ENP and the fabric when a water bridge is formed between the two substrates. They found that adhesion was strong between hydrophobic fabrics and ENPs that do not absorb water well. For example, they concluded that the release of ENPs increased for the cotton fabric. The cotton fabric is hydrophilic and absorbs water, therefore preventing a water bridge from forming on its surface and greatly reducing the ability of a capillary force to form between the cotton fabric and an ENP. From this conclusion, it can be hypothesized that cotton fabric would have an increased rate of penetration compared to the other fabrics due to the lack of capillary forces keeping the ENPs on the surface. This effect causes more particles to become resuspended from contaminated cotton surfaces, also indicating that when particles enter the pores of fabric, they would easily pass through. However, our results of penetration study showed that polypropylene actually failed to trap more ENPs compared to cotton and that cotton and polyester cotton performed similarly when challenged with both Al_2O_3 and CB. Therefore, capillary forces must not play a significant role in sticking ENPs to fabric surfaces when particles are moving through fabric with a similar velocity as demonstrated in this study. It is more likely that the fabric's porosity and packing density play a larger role in overall fabric efficiency than hydrophobic forces or capillary forces. Electrostatic interaction between particle and fabric was not discussed in this paper because it is believed that the face velocity that occurs at the face of the fabric when worn by a worker is too low for electrostatic forces to become a dominant trapping mechanism. Future research should focus on the surface charge of protective clothing fabrics and their role in trapping uncharged ENPs.

CONCLUSIONS

Four important conclusions can be drawn from this investigation. First, Tyvek fabric was shown to be the most protective. Tyvek consistently showed the lowest penetration percentages when challenged with all three different types of ENPs, and some results showed that Tyvek had a statistically significantly lower penetration than all three other fabrics. One potential issue to be considered regarding Tyvek fabric trapping the most ENPs onto the surface is the accumulation of ENPs loosely attached on the fabric surface causing resuspension of ENPs becoming airborne when the fabric was disturbed, shaken, or removed by the wearer. Second, polypropylene had the highest penetration percentages when challenged with CB and Al_2O_3 nanoparticles. This may be explained by the fact that polypropylene has the highest calculated porosity when compared with the other three fabrics, and the governing mode of deposition for particles of this size is interception. Polypropylene was the most nonhomogeneous fabric challenged, and it can be concluded that many ENPs could easily pass through the gaps in the fabric. Third, CNT nanoparticles penetrated all four fabrics significantly less than the other two ENPs studied. This may be due to the elongated fiber shape of a CNT fiber compared to the spherical shape of the other two particles and the high agglomeration rate of CNTs. Fourth, porosity and fabric structure are more important factors to consider when determining a fabric's overall filtration efficiency, while surface chemistry is less important. These conclusions can be helpful in determining which fabric will provide the greatest protection against certain ENPs with different physical and chemical characteristics.

ASSOCIATED CONTENT

Supporting Information

The Supporting Information is available free of charge at https://pubs.acs.org/doi/10.1021/acs.chas.4c00021.

SEM images of each fabric, upstream particle concentrations, calculations, and statistical analysis (PDF)

AUTHOR INFORMATION

Corresponding Author

Candace Su-Jung Tsai − *Department of Environmental Health Sciences, Fielding School of Public Health, University of California, Los Angeles, California 90095, United States;* orcid.org/0000-0002-7296-8278; Phone: (310) 206-9258; Email: candacetsai@ucla.edu

Authors

Natalie Ireland − *Department of Environmental Health Sciences, Fielding School of Public Health, University of California, Los Angeles, California 90095, United States*

Yi-Hsuan Chen − *Department of Environmental Health Sciences, Fielding School of Public Health, University of California, Los Angeles, California 90095, United States*

Complete contact information is available at: https://pubs.acs.org/10.1021/acs.chas.4c00021

Funding

This work was supported by the Department of Health and Human Services, Center for Disease Control and Prevention Grant No. 1 R21OH011507-01 and 5T42OH008412-16.

Notes

The authors declare no competing financial interest.

ACKNOWLEDGMENTS

The authors would like to thank Dr. Rachael Jones and Dr. Yifang Zhu at the Department of Environmental Health Sciences, University of California, Los Angeles, for reviewing and providing feedback on this manuscript.

REFERENCES

(1) Amoabediny, G. H.; Naderi, A.; Malakootikhah, J.; Koohi, M. K.; Mortazavi, S. A.; Naderi, M.; Rashedi, H. Guidelines for safe handling, use and disposal of nanoparticles. *J. Phys.: Conf. Ser.* **2009**, *170*, 012037.

(2) National Institute for Occupational Safety and Health. *Approaches to Safe Nanotechnology*; Centers for Disease Control and Prevention, 2009.

(3) National Institute for Occupational Safety and Health. *Building A Safety Program to Protect the Nanotechnology Workforce*; Centers for Disease Control and Prevention, 2016; Vol. *102*.

(4) Tsai, C. S.-J. Contamination and release of nanomaterials associated with the use of personal protective clothing. *Ann. Occup. Hyg.* **2015**, *59* (4), 491−503.

(5) Maksot, A.; Sorna, S. M.; Blevens, M.; Reifenberger, R. G.; Hiyoto, K.; Fisher, E. R.; Vindell, T.; Li, Y. V.; Kipper, M. J.; Tsai, C. S.-J. Engineered Nanoparticle Release from Personal Protective Clothing: Implications for Inhalation Exposure. *ACS Appl. Nano Mater.* **2022**, *5* (2), 2558−2568.

(6) Licina, D.; Nazaroff, W. W. Clothing as a transport vector for airborne particles: Chamber study. *Indoor Air* **2018**, *28* (3), 404−414.

(7) Monteiro-Riviere, N. A.; Nemanich, R. J.; Inman, A. O.; Wang, Y. Y.; Riviere, J. E. Multi-walled carbon nanotube interactions with

human epidermal keratinocytes. *Toxicol. Lett.* **2005**, *155* (3), 377−384.
(8) Palmer, B. C.; Phelan-Dickenson, S. J.; DeLouise, L. A. Multi-walled carbon nanotube oxidation dependent keratinocyte cytotoxicity and skin inflammation. *Part. Fibre Toxicol.* **2019**, *16* (1), 3−15.
(9) Shvedova, A.; Castranova, V.; Kisin, E.; Schwegler-Berry, D.; Murray, A.; Gandelsman, V.; Maynard, A.; Baron, P. Exposure to Carbon Nanotube Material: Assessment of Nanotube Cytotoxicity using Human Keratinocyte Cells. *J. Toxicol. Environ. Health, Part A* **2003**, *66* (20), 1909−1926.
(10) Crosera, M.; Bovenzi, M.; Maina, G.; Adami, G.; Zanette, C.; Florio, C.; Filon Larese, F. Nanoparticle dermal absorption and toxicity: a review of the literature. *Int. Arch. Occup. Environ. Health* **2009**, *82* (9), 1043−1055.
(11) Filipe, P.; Silva, J. N.; Silva, R.; Cirne de Castro, J. L.; Marques Gomes, M.; Alves, L. C.; Santus, R.; Pinheiro, T. Stratum Corneum Is an Effective Barrier to TiO2 and ZnO Nanoparticle Percutaneous Absorption. *Skin Pharmacol. Physiol.* **2009**, *22* (5), 266−275.
(12) Filon, F. L.; Bello, D.; Cherrie, J. W.; Sleeuwenhoek, A.; Spaan, S.; Brouwer, D. H. Occupational dermal exposure to nanoparticles and nano-enabled products: Part I—Factors affecting skin absorption. *Int. J. Hyg Environ. Health* **2016**, *219* (6), 536−544.
(13) Labouta, H. I. P.; Schneider, M. P. Interaction of inorganic nanoparticles with the skin barrier: current status and critical review. *Nanomedicine* **2013**, *9* (1), 39−54.
(14) Oberdorster, G.; Oberdorster, E.; Oberdorster, J. Nanotoxicology: An Emerging Discipline Evolving from Studies of Ultrafine Particles. *Environ. Health Perspect.* **2005**, *113* (7), 823−839.
(15) Liang, X. W.; Xu, Z. P.; Grice, J.; Zvyagin, A. V.; Roberts, M. S.; Liu, X. Penetration of Nanoparticles into Human Skin. *Curr. Pharmaceut. Des.* **2013**, *19* (35), 6353−6366.
(16) Menczel, E.; Maibach, H. I. In vitro human percutaneous penetration of benzyl alcohol and testosterone: epidermal-dermal retention. *J. Invest. Dermatol.* **1970**, *54* (5), 386−394.
(17) Golanski, L.; Guiot, A.; Rouillon, F.; Pocachard, J.; Tardif, F. Experimental evaluation of personal protection devices against graphite nanoaerosols: fibrous filter media, masks, protective clothing, and gloves. *Hum. Exp. Toxicol.* **2009**, *28* (6−7), 353−359.
(18) Lee, K. W.; Liu, B. Y. H. On the Minimum Efficiency and the Most Penetrating Particle Size for Fibrous Filters. *J. Air Pollut. Control Assoc.* **1980**, *30* (4), 377−381.
(19) Steffens, J.; Coury, J. R. Collection efficiency of fiber filters operating on the removal of nano-sized aerosol particles: I—Homogeneous fibers. *Sep. Purif. Technol.* **2007**, *58* (1), 99−105.
(20) Kim, S. C.; Wang, J.; Emery, M. S.; Shin, W. G.; Mulholland, G. W.; Pui, D. Y. H. Structural Property Effect of Nanoparticle Agglomerates on Particle Penetration through Fibrous Filter. *Aerosol. Sci. Technol.* **2009**, *43* (4), 344−355.
(21) Lange, R.; Fissan, H.; Schmidt-Ott, A. Predicting the Collection Efficiency of Agglomerates in Fibrous Filters. *Part. Part. Syst. Char.* **1999**, *16* (2), 60−65.
(22) Gao, P.; Jaques, P. A.; Hsiao, T.-C.; Shepherd, A.; Eimer, B. C.; Yang, M.; Miller, A.; Gupta, B.; Shaffer, R. Evaluation of Nano- and Submicron Particle Penetration through Ten Nonwoven Fabrics Using a Wind-Driven Approach. *J. Occup. Environ. Hyg.* **2011**, *8* (1), 13−22.
(23) He, M.; Ghee, T. A.; Dhaniyala, S. Aerosol penetration through fabrics: Experiments and theory. *Aerosol. Sci. Technol.* **2021**, *55* (3), 289−301.
(24) Jamriska, M. *Aerosol Penetration through Protective Fabrics*; Human Protection and Performance Division, 2009.
(25) Rengasamy, S.; Eimer, B.; Shaffer, R. E. Simple Respiratory Protection—Evaluation of the Filtration Performance of Cloth Masks and Common Fabric Materials Against 20−1000 nm Size Particles. *Ann. Occup. Hyg.* **2010**, *54* (7), 789−798.
(26) Konda, A.; Prakash, A.; Moss, G. A.; Schmoldt, M.; Grant, G. D.; Guha, S. Aerosol Filtration Efficiency of Common Fabrics Used in Respiratory Cloth Masks. *ACS Nano* **2020**, *14* (5), 6339−6347.
(27) Faccini, M.; Vaquero, C.; Amantia, D. Development of Protective Clothing against Nanoparticle Based on Electrospun Nanofibers. *J. Nanomater.* **2012**, *2012*, 1−9.
(28) Hiyoto, K.; Sorna, S. M.; Maksot, A.; Reifenberger, R. G.; Tsai, C. S.-J.; Fisher, E. R. Effects of Surface Hydrophobicity of Lab Coat Fabrics on Nanoparticle Attachment and Resuspension: Implications for Fabrics Used for Making Protective Clothing or Work Uniform. *ACS Appl. Nano Mater.* **2023**, *6* (9), 7384−7394.
(29) Wingert, L.; Cloutier, Y.; Hallé, S.; Bahloul, A.; Tessier, D.; Giraudel, J.-L.; Dolez, P.; Tuduri, L. Filtering performances of 20 protective fabrics against solid aerosols. *J. Occup. Environ. Hyg.* **2019**, *16* (8), 592−606.
(30) Bahgat, M.; Farghali, A. A.; El Rouby, W. M. A.; Khedr, M. H. Synthesis and modification of multi-walled carbon nano-tubes (MWCNTs) for water treatment applications. *J. Anal. Appl. Pyrolysis* **2011**, *92* (2), 307−313.
(31) Dhineshbabu, N. R.; Mahadevi, N.; Assein, D. Electronic applications of multi-walled carbon nanotubes in polymers: A short review. *Mater. Today: Proc.* **2020**, *33*, 382−386.
(32) Khodabakhshi, S.; Fulvio, P. F.; Andreoli, E. Carbon black reborn: Structure and chemistry for renewable energy harnessing. *Carbon* **2020**, *162*, 604−649.
(33) Svegl, I. G.; Bele, M.; Ogorevc, B. Carbon black nanoparticles film electrode prepared by using substrate-induced deposition approach. *Anal. Chim. Acta* **2008**, *628* (2), 173−180.
(34) Loeb, S.; Li, C.; Kim, J.-H. Solar Photothermal Disinfection using Broadband-Light Absorbing Gold Nanoparticles and Carbon Black. *Environ. Sci. Technol.* **2018**, *52* (1), 205−213.
(35) Cheng, J.; Sun, Z.; Yu, Y.; Li, X.; Li, T. Effects of modified carbon black nanoparticles on plant-microbe remediation of petroleum and heavy metal co-contaminated soils. *Int. J. Phytoremediation* **2019**, *21* (7), 634−642.
(36) Ingham, C. J.; ter Maat, J.; de Vos, W. M. Where bio meets nano: the many uses for nanoporous aluminum oxide in biotechnology. *Biotechnol. Adv.* **2012**, *30* (5), 1089−1099.
(37) Jwad, K. H.; Saleh, T. H.; Abd-Alhamza, B. Preparation of Aluminum Oxide Nanoparticles by Laser Ablation and a Study of Their Applications as Antibacterial and Wounds Healing Agent. *Nano Biomed. Eng.* **2019**, *11* (3), 313−314.
(38) Maquieira, A.; Brun, E. M.; Garcés-García, M.; Puchades, R. Aluminum Oxide Nanoparticles as Carriers and Adjuvants for Eliciting Antibodies from Non-immunogenic Haptens. *Anal. Chem.* **2012**, *84* (21), 9340−9348.
(39) Lo, S.-I.; Chen, P.-C.; Huang, C.-C.; Chang, H.-T. Gold Nanoparticle-Aluminum Oxide Adsorbent for Efficient Removal of Mercury Species from Natural Waters. *Environ. Sci. Technol.* **2012**, *46* (5), 2724−2730.
(40) Gumus, S.; Ozcan, H.; Ozbey, M.; Topaloglu, B. Aluminum oxide and copper oxide nanodiesel fuel properties and usage in a compression ignition engine. *Fuel* **2016**, *163*, 80−87.
(41) NanoLab. MultiWalled Carbon Nanotube Safety Data Sheet, 2017. https://www.nano-lab.com/nanotubes-research-grade.html (accessed May 13, 2024).
(42) MSESupplies. MSE PRO 30 nm High Purity 99.99% Alpha Aluminum Oxide Nanoparticles, 2024. https://www.msesupplies.com/products/mse-pro-30-nm-high-purity-99-99-alpha-aluminum-oxide-nanoparticles?variant=48150436431 (accessed May 13, 2024).
(43) Carbons, O. E. Carbon Black, 2022. https://orioncarbons.com/orion/safety/safety-data-sheets/ (accessed May 13, 2024).
(44) Birch, M. E.; Wang, C.; Fernback, J. E.; Feng, H. A.; Birch, Q. T.; Dozier, A. K. Analysis of carbon nanotubes and nanofibers on mixed cellulose ester filters by transmission electron microscopy. *NIOSH Manual of Analytical Methods*, 5th ed.; Department of Health and Human Services, Centers for Disease Control and Prevention, National Institute for Occupational Safety and Health, DHHS (NIOSH) Publication: Cincinnati, 2017.
(45) Wiedensohler, A.; Birmili, W.; Nowak, A.; Sonntag, A.; Weinhold, K.; Merkel, M.; Wehner, B.; Tuch, T.; Pfeifer, S.; Fiebig, M.; et al. Mobility particle size spectrometers: harmonization of

technical standards and data structure to facilitate high quality long-term observations of atmospheric particle number size distributions. *Atmos. Meas. Tech.* **2012**, *5* (3), 657−685.
(46) Wiedensohler, A.; Wiesner, A.; Weinhold, K.; Birmili, W.; Hermann, M.; Merkel, M.; Müller, T.; Pfeifer, S.; Schmidt, A.; Tuch, T.; et al. Mobility particle size spectrometers: Calibration procedures and measurement uncertainties. *Aerosol. Sci. Technol.* **2018**, *52* (2), 146−164.
(47) Liu, P. S. K.; Deshler, T. Causes of Concentration Differences Between a Scanning Mobility Particle Sizer and a Condensation Particle Counter. *Aerosol. Sci. Technol.* **2003**, *37* (11), 916−923.
(48) Hinds, W. C.; Zhu, Y. *Aerosol Technology: Properties, Behavior, and Measurement of Airborne Particles*; John Wiley & Sons, 2022.
(49) Dhaniyala, S.; Liu, B. Y. H. Theoretical Modeling of Filtration by Nonuniform Fibrous Filters. *Aerosol. Sci. Technol.* **2001**, *34* (2), 170−178.
(50) Wang, J.; Kim, S. C.; Pui, D. Y. H. Measurement of multi-wall carbon nanotube penetration through a screen filter and single-fiber analysis. *J. Nanoparticle Res.* **2011**, *13* (10), 4565−4573.
(51) Chen, S.-C.; Wang, J.; Bahk, Y. K.; Fissan, H.; Pui, D. Y. H. Carbon Nanotube Penetration Through Fiberglass and Electret Respirator Filter and Nuclepore Filter Media: Experiments and Models. *Aerosol. Sci. Technol.* **2014**, *48* (10), 997−1008.
(52) Pashley, R. M.; McGuiggan, P. M.; Ninham, B. W.; Evans, D. F. Attractive Forces between Uncharged Hydrophobic Surfaces: Direct Measurements in Aqueous Solution. *Science* **1985**, *229* (4718), 1088−1089.
(53) Faghihnejad, A.; Zeng, H. Interaction Mechanism between Hydrophobic and Hydrophilic Surfaces: Using Polystyrene and Mica as a Model System. *Langmuir* **2013**, *29* (40), 12443−12451.
(54) Ducker, W. A.; Mastropietro, D. Forces between extended hydrophobic solids: Is there a long-range hydrophobic force? *Curr. Opin. Colloid Interface Sci.* **2016**, *22*, 51−58.

https://doi.org/10.1021/acs.chas.4c00021
ACS Chem. Health Saf. 2024, 31, 393−403